Creep Deformation of Compacted Decomposed Granite Soils

Sukeo O-HARA* and Hiroshi MATSUDA*

(Received July 14, 1984)

Abstract

In order to investigate the characteristics of time dependent deformation on the decomposed granite soils, the drained triaxial compression tests were performed under loading the constant deviator stress. In this study, two kinds of samples with different grain size distributions were prepared to investigate the effects of the grain size and the particle crushing on the deformation.

As a result, it was observed that there existed the creep deformations on the compacted sample, and especially in the creep tests, whether the specimen attained the failure or not was essentially different ; in the former case, the dilatancy increases and in the latter case, the shrinkage does.

Introduction

Decomposed granite soils are distributed widely in the western of Japan and used frequently as the materials of earth structures such as embankment and reclaimed land. In the construction on such a ground surface, the strip footings instead of the pile foundations are ordinary employed because of the difficulty of pile driving due to a coarse fraction included in the soil. So, the investigation of the creep deformation are necessary to predict the stability of the ground over a long period of time.

For the creep deformation characteristics of the decomposed granite soil, it has been observed that there existed a creep deformation during drained triaxial tests on the rocky sample[1] and the time dependent settlement continued after immediate compression on the undisturbed and considerably weathered sample[2]. Matsuura et al[3]. investigated that curves of the settlement versus log of time in the plate bearing tests on the sample with different degree of weathering were approximated by straight lines. Thus the remarkable creep deformations have been observed on the decomposed granite soil, but there are many facts which have not been clarified.

In this study, the relationships between the axial or volumetric strain and elapsed time were obtained in the drained triaxial tests and then these relationships were examined in order to reveal the characteristics of time dependent deformation of the decomposed granite soils.

Especially, the effects of the grain size and the particle crushing on the deformation were examined using the specimen with different grain size distributions.

* Department of Civil Engineering.
** Department of Construction Engineering.

Sample and specimen

A soil used in this study is decomposed granite soils taken from the housing site in Ube city area, western Japan.

The specific gravity of this sample G_s is 2.670, the optimum moisture content w_{opt} and the maximum dry density γ_{dmax} obtained by the compaction tests are 13.8%, 18.24kN/m^2, respectively. In addition, the maximum grain size D_{max} and the uniformity coefficient U_c are 10.0mm, and 15.0.

In this study, from this natural soils two kinds of samples were prepared for testing ; one is obtained by eliminating a coarse fraction larger than 2000 μm and the other is obtained by eliminating a coarse fraction larger than 840 μm. In this paper, the former is designated as "Sample Ⅰ", and the latter as "Sample Ⅱ". The grain size distribution curves of them are also shown in Fig. 1.

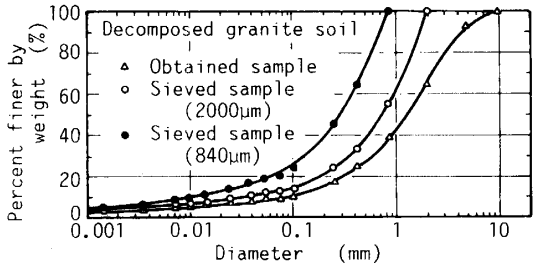

Fig. 1 Grain size distributions of tested sample.

To make a specimen of a size 35mm in diameter and 70mm high, after the moisture content of these samples were adjusted to 13.8% for the sample Ⅰ, and 12.9% for the sample Ⅱ, they were put into the mold divided into three layers, and each layer was compacted 25 times with the tamping bar. In this case, the reason why the moisture content was varied between the sample Ⅰ and the sample Ⅱ is to obtain the void ratio in the region of 0.78－0.81 and the degree of saturation in the region of 43%－47%.

For these specimens, the stress controlled triaxial compression tests were performed under the respective confining pressure of 29.4, 49.0, 98.0kN/m^2. The increment of the axial load, the sum of which would lead the specimen to the failure (which is defined as the axial of 15%) in about 90 minutes, was applied every 5 minutes. As a result, the internal friction angle of $\phi = 39.4°$, the cohesion of c = 3.72kN/m^2 were obtained and to normalize the constant deviator stress in the creep test the shear strength at the failure conditions was decided as follows ; σ_d = 114.6kN/m^2 for the sample Ⅰ, σ_d=172.2kN/m^2 for the sample Ⅱ, respectively.

Apparatus

In Fig. 2, the outline of the triaxial apparatus is diagramatically shown. A series

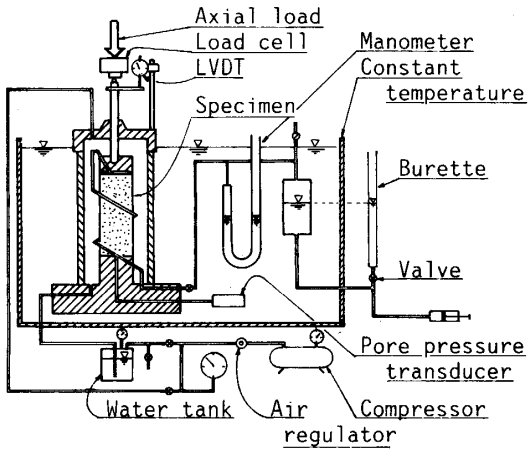

Fig. 2 Outline of the triaxial apparatus.

of tests were performed under the conditions of drainage from the upper boundary of the specimen and the constant confining pressure. The volume change of the specimen was obtained by measuring the change of the water head in the burette which was moved up or down continually to maintain the liquid head in the manometer constant.

Since a test was continued for a long time, the triaxial cell and the tube including the air drained from the specimen was sunk into the constant temperature (20°C) water bath in order to reduce the effect of the change of temperature on the volume change of the air included in the specimen and on the deformation characteristics of the specimen.

The confining pressure was applied to the specimen with the regulated air after filling the triaxial cell with the water. The axial load was applied by using the loading system of the standard oedommeter test apparatus.

The change of the axial load and the pore pressure at the lower boundary were measured with the load cell and the pressure transducers and these were recorded automatically with the pen recorder. As for the pore pressure, however, the effect of the change of it was neglected because the value obtained in the every test was less than 3% of the confining pressure.

The specimen was primarily consolidated under the isotropic pressure for 1 hour and then sheared under the loading conditions of the predetermined deviator stress, which was kept constant by correcting the axial load using the measured axial and volumetric strain.

Test results

Typical relationships between the axial strain and the log of elapsed time on the sample Ⅰ and the sample Ⅱ obtained in the triaxial compression tests under the constant deviator stress are shown in Fig. 3. In each curve it is observed that a large

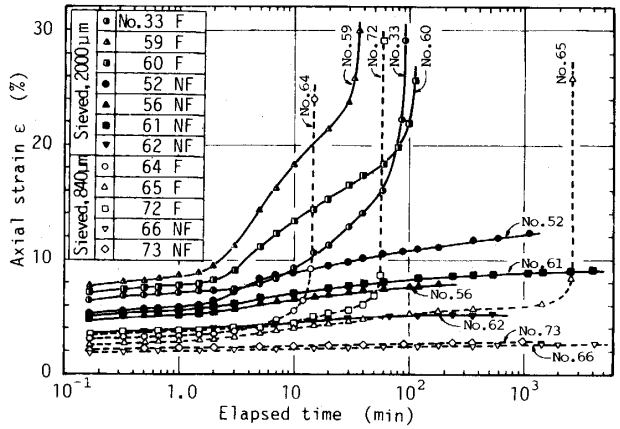

Fig. 3 Axial strain-time curves of compacted decomposed granite soils.

axial strain is produced immediately after the loading, especially this fact is remarkably produced in sample Ⅰ more than in sample Ⅱ, and this indicates that the soil including the comparatively large particles in size causes larger immediate settlement. Then the axial strain increases gradually together with the lapse of time. Though it has been shown that in the undisturbed decomposed granite soils the time

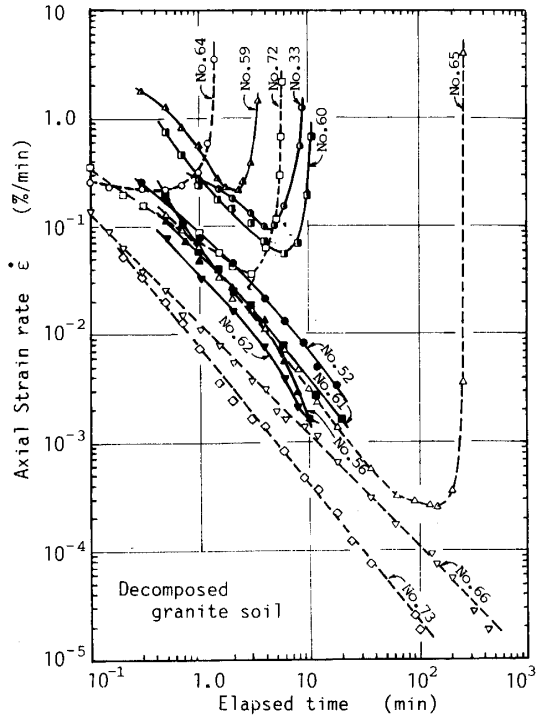

Fig. 4 Changes of axial strain rate with increasing the elapsed time in drained triaxial compression test.

dependent deformation was caused, in the current paper it was indicated that in the disturbed samples the similar deformation was also caused.

Furthermore, although several curves for the specimens that finally attained the failure conditions are shown in Fig. 3, the shape of them is different between the sample I and the sample II ; for the sample I the axial strain starts to increase gradually from the early stage after loading, but for the sample II the axial strain increases abruptly after some period of time, similar to the curve[4] obtained in the drained triaxial tests on the cohesive soil.

The typical relationships between the axial strain rate and elapsed time are shown on the logarithmic diagram in Fig. 4. As for the specimen attained the failure condition, the strain rate decreases linearly with elapsed time and after passing through the minimum strain rate, it contrarily increases. For the specimen not attained the failure condition, the continuous reduction in strain rate is observed instead of the existence of the minimum strain rate.

Singh, Mitchell[5] indicate that the axial strain rate at any time is given by

$$\dot{\varepsilon} = \dot{\varepsilon}_0 \exp(\alpha \cdot D)(t_1/t)^m \tag{1}$$

where D is the creep stress ratio defined by the ratio of the constant deviator stress to the shear strength of the specimen, and $\dot{\varepsilon}_0$ is the temporary axial strain rate in the case of D=0 and t=t_1. m is the material constant given by

$$m = -(d \log \dot{\varepsilon}) / (d \log t) \tag{2}$$

and indicates that the greater the absolute value of m increases, the larger the gradient of the linear portion of the curve in Fig. 4 becomes. The parameter α which indicates the slope of the linear portion of the logarithmic strain rate versus deviator stress plots is given by

$$\alpha = (d \log \dot{\varepsilon}) / (d D) \tag{3}$$

The relationships between the creep stress ratio D and m are shown in Fig. 5, in which the symbols are used as follows ; the solid symbols are for the specimen attained the failure condition and the open symbols for not attained it. As for the specimen finally attained the failure condition, m is obtained from the curves as far as the minimum strain rate occurs. In this case the apparent tendency is not recognized because of the scattering of the data varied from 0.6 to 1.4. For the specimen not attained the failure condition, however, in spite of a little scattering it is seen that m is rather constant rainging from 1.0 to 1.3.

The effect of the differences between the sample I and the sample II on the value of m is not observed in Fig. 5, but it is noticed that the creep stress ratio D which leads the specimen to failure is 98% for sample I and 94% for sample II . This indicates that the creep stress ratio D reduces with a reduction of the particle

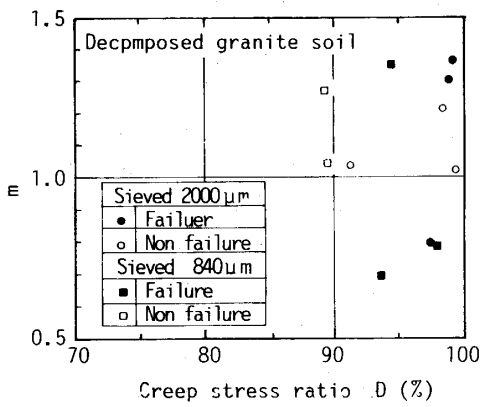

Fig. 5 Relationships between the creep stress ratio D and m which is obtained from the gradient of the linear portion of the curve in Fig. 4

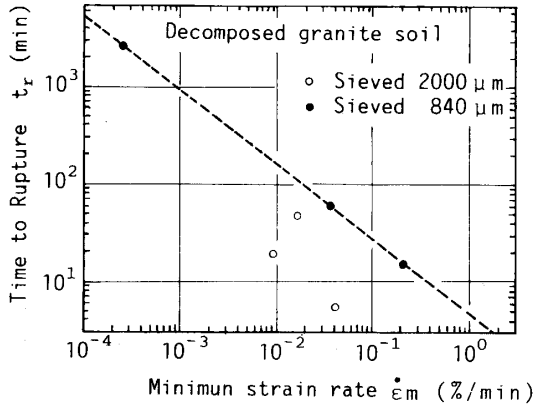

Fig. 6 Relationships between the elapsed time to cause a failure and the minimum strain rate.

size.

For the purpose of predicting the creep failure, Fig. 6 shows the relationships between the elapsed time t_r until the specimen attains the failure and the minimum strain rate. For the sample II the linear relations are observed and it can be expressed by

$$\log t_r = A - B \log \dot{\varepsilon}_m \tag{4}$$

where A (=0.652), B (=0.771) are constants. From this, it is noticed that the elapsed time t_r until attaining a failure condition increases with a reduction of the minimum strain rate $\dot{\varepsilon}_m$. For the sample I such relations can not be seen because of a large amount of scatter, but the reduction of the value B is observed from the location of

the plots under the ones for the sample Ⅱ. In the undrained creep tests on the cohesive soils, it has been shown[4] that there were the linear relations between t_r and $\dot{\varepsilon}_m$ and the value of B was approximately equal to 1.0. In accordance with the fact mentioned above, it is considered that the value of B decreases with an increase of the relative particle size.

Fig. 7 illustrates the change in the axial strain ε and minimum strain rate $\dot{\varepsilon}_m$. It is observed that for the sample Ⅱ the axial strain is almost constant regardless of the

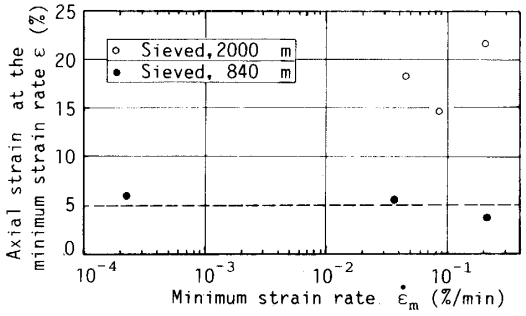

Fig. 7 Changes in axial strain and minimum strain rate.

minimum strain rate as seen in the undrained triaxial tests on cohesive soils. From this, it is noticed that the creep failure is caused by the yielding of the specimen at a certain axial strain which is not affected by the creep stress ratio.

The variations of the volumetric strain with an increase of time are illustrated on the semilog diagram in Fig. 8. For a certain period of time after loading, only a little amount of volumetric strain is observed. Then for the specimen attained the failure finally, the dilatancy develops abruptly after some additional period of time, but for the specimen not attained the failure condition, a tendency of volumetric shrikage is appeared after 500 — 1000min. Thus it is indicated that in the volume change there are apparent differences between the specimens finally attained and not attained the failure condition.

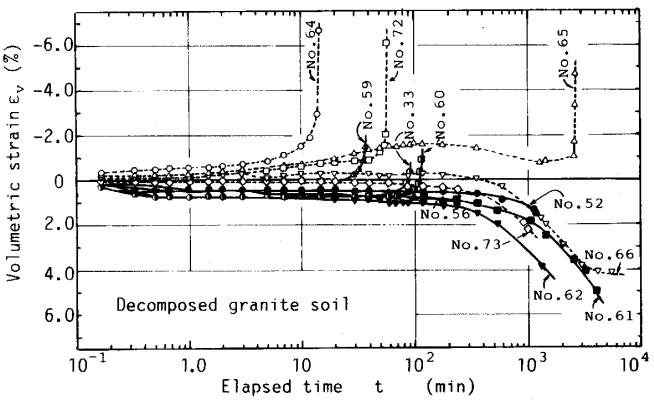

Fig. 8 Variations of volumetric strain with an increase of time.

Fig. 9 shows the relationships between the volumetric strain and the axial strain. As seen in Fig. 8, for the specimen not attained the failure condition, the volumetric shrinkage increases remarkably at a small axial strain and for the specimen attained the failure condition the dilatancy increases, especially in proportion to the axial

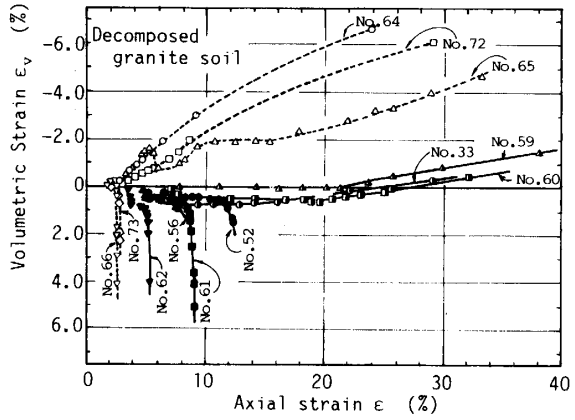

Fig. 9 Relationships between volumetric strain and axial strain.

strain when the axial strain is small. In comparison sample I with sample II, it can be seen that the amount of the dilatancy is larger in sample II than in sample I. In accordance with the fact[6] that in the drained triaxial test on sand with uniform particle size, the more the particle size reduces, the more the coefficient of dilatancy (the ratio of the increment of volumetric strain to that of axial strain) increases, we can understand the experimental results obtained herein.

As mentioned above, it was found out that the apparent creep deformation occured on the decomposed granite soil. As for the creep deformation of the granular soils without cohesion, a few experimental studies concerning the particle crushing phenomenon under the high confining pressure have been performed[7].

Marsal[8] introduced the value of B to appreciate the particle crushing phenomenon ; B is the sum of the positive Δi, where Δi is the difference between the percentage retained in a given sieve before and after compression test. So, in this study the mechanical analysis of specimens were performed after compaction and the shear test, and it was shown that a little particle crushing might occur because of the obtained value of B being 2 to 4. As comparing the deformation characteristics on sample I and sample II, however, since the latter is more similar to that of the cohesive soils, further study on the effects of the cohesion should be performed.

Conclusions

On a compacted decomposed granite soil, drained triaxial compression tests were performed to investigate the creep deformation characteristics and the following con-

clusions were obtained.

1) Creep deformations were observed on the compacted decomposed granite soil.

2) On the logarithmic diagram, curves of strain rate versus elapsed time after applying a constant deviator stress were approximated by linear lines for the specimen not attained the failure condition and for the specimen attained the failure one, and there existed a minimum strain rate at a constant axial strain independent of the creep stress ratio. This kind of deformation characteristics are similar to the ones in the undrained triaxial creep tests on chesive soils.

3) The characteristics of volumetric strain during creep tests for the specimen attained the failure condition or not are essencially different ; in the former case, the dilatancy increases and in the latter case, the volumetric shrinkage does.

Acknowagement

The authors would like to acknowledge Mr. F. Moriwaki for his help throughout this experimental work.

References

1) Akai K. et al. "Deformation Characteristics for a Long Period of Time as a Rock-Bed Foundation of Big Bridges", Proc., 30th Annual Meeting of JSCE, Part 3, 254–255 (1975)(in Japanese).

2) Nishida K. et al. "Characteristics for the Engineering and its Application of the Decomposed Granite Soil and Masa soils", Edited by JSSMFE, 185–192 (1982)(in Japanese).

3) Matsuura M. et al. "The Realities of Obstacles in the uneven Settlement at the Masa Soil Region", Report for the Research Grant of the Ministry of Education, 6–36 (1976) (in Japanese).

4) Aboshi H. and T. Moriwaki "Study on the Creep Deformation and Rupture under Undrained Conditions on a Saturated Clay", Technical Reports of Hiroshima University, **31**, 97–104 (1973) (in Japanese).

5) Singh A. and J. K. Mitchell "General Stress-Strain Time Function for Soils", ASCE **94**, 21–46 (1968).

6) Kirkpatrick W. M. "Effects of Grain Size and Grading on the Shearing Behavior of Granular Materials", Proc. 6th ICSMFE, **1**, 273–277 (1965).

7) Miura N. and T. Yamanouchi, "The Effect of the Particle-Crushing on the Shear Characteristics of a Sand", Proc. JSCE, **260**, 109–118 (in Japanese).

8) Marsal R. J. "Large Scale Testing of Rockfill Materials", ASCE, **93**, 27–43 (1967).